Santamaría-Orozco, D., and B. Horsfield, 2003, Gas generation potential of upper Jurassic (Tithonian) source rocks in the Sonda de Campeche, Mexico, *in* C. Bartolini, R. T. Buffler, and J. Blickwede, eds., The Circum-Gulf of Mexico and the Caribbean: Hydrocarbon habitats, basin formation, and plate tectonics: AAPG Memoir 79, p. 349–363.

Gas Generation Potential of Upper Jurassic (Tithonian) Source Rocks in the Sonda de Campeche, Mexico

Demetrio Santamaría-Orozco
Instituto Mexicano del Petróleo, Exploración, Mexico City, Mexico

Brian Horsfield
GeoForschungsZentrum, Potsdam, Germany

ABSTRACT

In the Sonda de Campeche offshore region of Mexico, the Tithonian sedimentary sequence is the most important source of hydrocarbons that occur today in Paleocene traps. The maturity of both source rocks and petroleum in reservoirs is known to increase from northeast to southwest across the region. This is manifested at the molecular level and in bulk petroleum properties such as API gravity and gas-oil ratio (GOR). We have analyzed a selection of source-rock samples from across the area, covering the entire maturity spectrum, by pyrolysis gas chromatography. These data give insights into the GOR of yet-to-be-generated petroleum for each maturity stage. A mass-balance model based on these same data and complementary data from laboratory experiments (MSSV pyrolysis) provided cumulative GOR as a function of generation stage (transformation ratio). Regional field GOR trends are consistent with instantaneous rather than cumulative GOR predictions, thereby supporting the notion of mainly localized vertical migration avenues in association with a late timing of trap formation.

INTRODUCTION AND GOALS

The Sonda de Campeche is part of the offshore portion of the Sureste Basin (Figure 1) and represents one of most prolific oil-producing areas of Mexico. The stratigraphic sequence consists of Jurassic to Holocene sediments (González and Holguín, 1991, 2001), and the tectonic style is extensional, leading to the development of half grabens and horst blocks. The sequence is a textbook example of a petroleum system in which high volumes of hydrocarbons have migrated vertically, being described as a ''supercharged, high impedance petroleum system'' by Demaison and Huizinga (1994).

The major source rock is of Tithonian age, consisting of massive black shales and dark-gray, clayey, laminated shales deposited on an anoxic marine-carbonate shelf (Angeles-Aquino, 1987). The Tithonian source rock has an average thickness of 220 m (Santamaría et al., 1997). Previous studies indicate that the Tithonian sequence has the highest organic matter content of the stratigraphic column with more than 2% wt of TOC, that it contains type II kerogen rich in sulfur, and that it has suffered different degrees

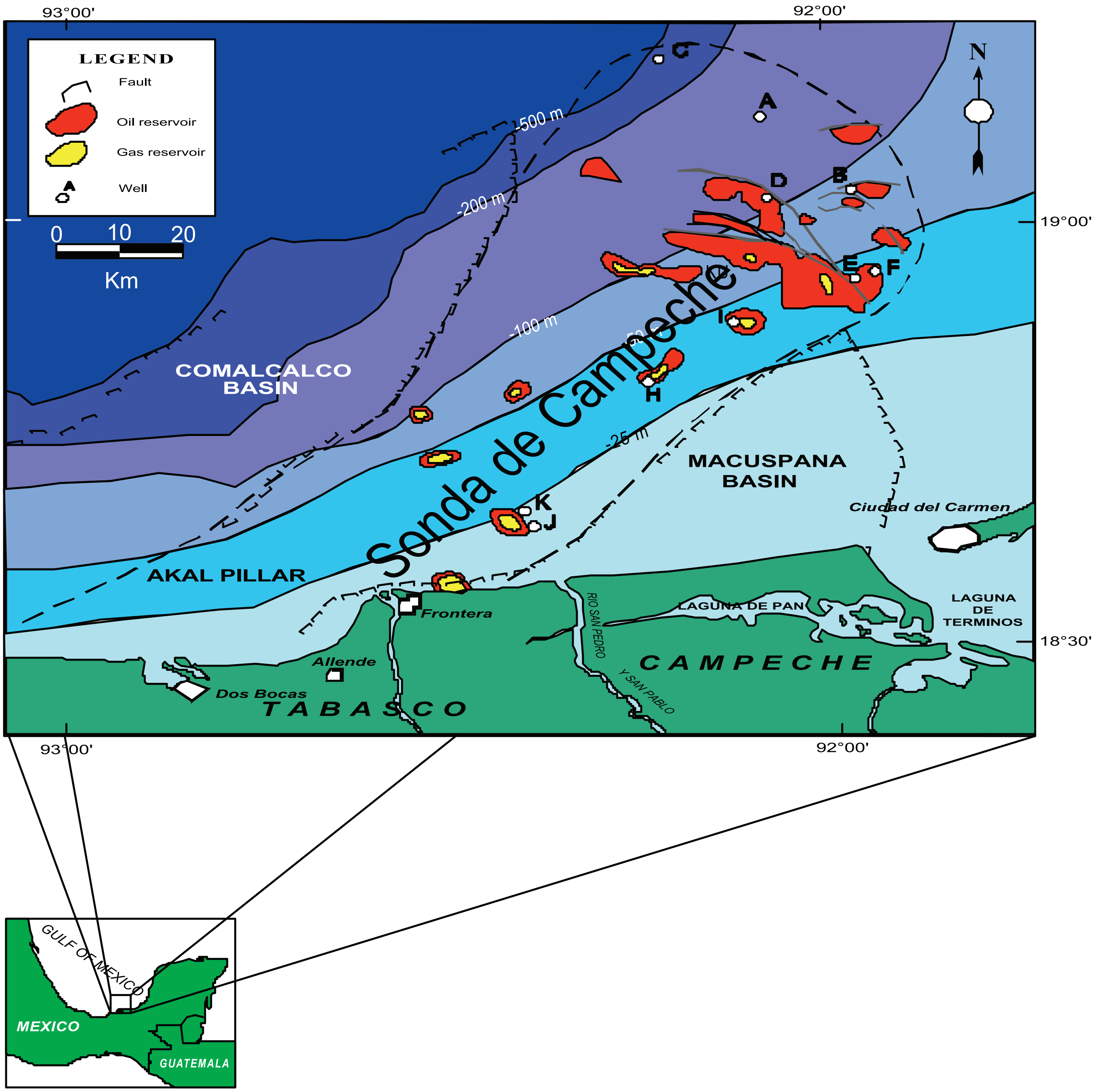

Figure 1. Location of the study area. The bold dashed line shows the limit of the Sonda de Campeche, and the segmented lines show the main fault zones.

of thermal evolution (Holguín, 1987; Santamaría et al., 1995; Sosa, 1995, Ortega et al., 1996; Santamaría et al., 1998; Romero et al., 1999; Ortuño, 1999). While some variability in organofacies is evident from organic petrological studies (Santamaría et al., 1995), it is manifested only to a small extent in bulk chemical properties. Indeed, maturity is the overriding control in determining the composition of generated hydrocarbons, as documented by progressively decreasing hydrogen indices and the appearance of a classical "oil window" defined by yields of soluble organic matter (Santamaría et al., 1998, and references therein).

Previous work has concentrated on oil generation as a function of maturity. The aforementioned publications reported that source-rock maturity increases from north to south. In the northern part of the area, vitrinite reflectance values are< 0.45% R_o, whereas the central part is mature (>0.5 < 1.0% R_o), coinciding with the highest oil production. The southern area is overmature, as shown by vitrinite reflectance values greater than 1.0% R_o. Only light oils, gas, and condensates are found in the southern area. The current study aims to quantify the relative proportions of oil and gas generated from organic matter of the Tithonian sequence during successive thermal evolution stages. To this end, a compositional mass-balance model using analytical pyrolysis data and product yields from artificial maturation experiments (MSSV pyrolysis) were employed.

SAMPLES AND METHODS

Geochemical screening analyses, including LECO and Rock Eval, followed by extraction and separation in the fractions of saturated, aromatics, and NSO (nitrogen, sulfur, oxygen) compounds (Santamaría et al., 1998) were done on core samples from 10 wells of the Sonda de Campeche that were considered representative of the Tithonian in the study area, based on their petroleum potential and maturity stage (Tables 1 and 2).

Pyrolysis gas chromatography (PyGC) was performed on whole rock samples and kerogen concentrates using a system similar to the one described by Horsfield and Düppenbecker (1991). Kerogen concentrates were obtained following the procedure described by Durand and Nicaise (1980). Briefly stated, the rock powder, after bitumen extraction, was treated with hot hydrochloric and hydrofluoric acids (at 70°C) in order to dissolve carbonate and silicate minerals, resulting in an enrichment of the organic matter. Approximately 2 mg of powdered kerogen concentrate (higher amounts for whole-rock samples) was heated in a helium atmosphere (30 ml/min). Products that released up to 300°C were vented (ambient to 300°C at ballistic heating rate, 300°C held for 3 min). Products generated during heating from 300° to 600°C (40°C/min, held 600°C for 2 min) were collected in a cryogenic trap (liquid nitrogen cooling). Trapped products were liberated by removing the cooling agent and heating the trap to 300°C. The released products were analyzed by gas chromatography (GC). The GC used was a HP 5890 Series II equipped with a fused silica capillary column (BP-1) of 25 m length and 0.3 mm internal diameter and coated with dimethylpolysiloxane of 0.32 μm film thickness. The GC oven temperature was programmed from 40° to 320°C at 8°C/min. Compounds generated were detected, once quantified, using a flame ionization detector and an external butane standard. Yields of boiling ranges (C_1–C_5, C_6–C_{14}, and C_{15+}), compound types (e.g., aliphatic hydrocarbons, aromatic hydrocarbons) and individual components were used in the mass-balance calculations.

Pyrolysis gas chromatography–mass spectrometry (PyGC-MS) was performed in order to identify the compounds generated from the kerogen samples. The analyses were performed using a Fisons Mass Lab mass spectrometer coupled to a Fisons GC 800 equipped with a fused silica capillary column (HP 1) of 50 m length and a 0.3 mm internal diameter coated with dimethylpolysiloxane of 0.5 μm film thickness. Products that released up to 300°C were vented (ambient to 300°C at ballistic heating rate, 300° held for 5 min). Products generated during the heating from 300° to 600°C (40°C/min, held 600°C for 2 min) were collected in a cryogenic trap (liquid nitrogen cooling). Trapped products were liberated by removing the cooling agent and heating the trap to 300°C. The GC oven temperature was programmed from 40° to 320°C at 8°C/min.

Table 1. TOC and Rock-Eval data of the Tithonian samples from all wells. Well locations are shown in Figure 1.

Well	*Rock Sample*	*TOC %*	*$CaCO_3$ %*	*S_1 mg/g*	*S_2 mg/g*	*S_3 mg/g*	*T max °C*	*PI*	*HI*	*OI*	*Lithology*
A	E-41495	22.80	3.33	4.96	171.57	1.97	409	0.03	753	9	Shale
B	E-41502	4.41	67.42	0.89	29.88	0.81	415	0.03	678	18	Shaly limestone
C	E-41525	5.02	44.83	0.92	30.41	2.65	414	0.03	606	53	Marl
D	E-41449	4.60	64.17	5.06	23.56	0.25	435	0.18	512	5	Marl
F	E-41459	5.00	16.58	6.31	16.85	0.40	433	0.27	337	8	Shale
G	E-41466	2.96	82.00	5.09	11.55	0.33	429	0.31	390	11	Shaly limestone
H	E-41488	3.40	40.92	3.40	11.41	0.31	436	0.23	336	9	Marl
I	E-41440	1.42	53.17	0.85	1.44	0.23	436	0.37	101	16	Marl
J	E-41500	3.02	83.17	0.74	2.49	0.19	452	0.23	82	6	Shaly limestone
K	E-41509	3.66	45.25	1.27	1.55	0.28	467	0.45	42	8	Marl

Table 2. Additional bulk geochemical and petrographic characteristics of Tithonian source rocks. Well locations are shown in Figure 1.

Well	*Number*	*Extract mg/g TOC*	*Sat mg/g TOC*	*Aro mg/g TOC*	*NSO mg/g TOC*	*not recovered mg/g TOC*	*R_o%*	*S/C*	*Liptinite %*	*Vitrinite %*	*Inertinite %*
A	E-41495	91	<1	3	20	67	0.35	0.30	77	18	5
B	E-41502	75	3	10	34	27	0.36	0.29	91	7	2
C	E-41525	45	2	3	16	24	0.38	0.55	88	8	4
D	E-41449	836	79	198	374	185	0.49	0.29	89	9	2
F	E-41459	676	146	119	272	139	0.65	0.53	92	6	2
G	E-41466	792	118	167	343	165	0.75	n.d.	93	5	2
H	E-41488	492	102	95	185	109	0.85	0.49	91	7	2
I	E-41440	208	71	39	44	54	0.91	1.35	94	3	3
J	E-41500	49	14	10	8	17	1.09	0.17	90	5	5
K	E-41509	44	20	57	5	13	1.29	0.57	87	6	7

One multistep PyGC experiment was performed on an immature Tithonian source-rock sample (R_o = 0.35%) in order to establish the thermal labilities of primary gas-forming and oil-forming substituents. Approximately 2 mg of preextracted kerogen concentrate was heated under a constant helium flow (50 ml/min) up to 300°C (ballistic heating rate, 300°C held constant for 10 min). All released products were vented. Pyrolysis then was performed in five temperature steps (PyGC[5]) following the procedure described by di Primio and Horsfield (1996). The temperature stages used in this experiment (following the same procedure described above) were 300–375°C, 375–400°C, 400–425°C, 425–450°C, and 450–600°C.

Microscale sealed-vessel pyrolysis (MSSV, Horsfield et al., 1989) was performed on a preextracted kerogen concentrate sample of low maturity (R_o = 0.35%) in order to measure the formation of oil and gas as a function of thermal stress. For each experiment, a glass capillary tube (100 μl internal volume) was flexed (120° angle), trimmed to approximately 40μl volume, and then sealed at one end. Precleaned glass beads (80–120 mesh) were added up to the level of the elbow in the sealed arm of the tube. Between 1 and 5 mg of kerogen was weighed into the tube. The internal volume then was reduced to about 10 μl by filling the remainder of the tube with thermally precleaned glass beads. A heating rate of 0.7 Kelvin/min was employed for the pyrolysis with seven samples being taken at 300°, 320°, 340°, 360°, 380°, 400°, and 450°C on each sample. Product yields were calculated using an external butane standard. The transformation ratio for any given experiment was defined as the ratio of total products at that temperature divided by the maximum yield of products seen at the highest temperature.

RESULTS AND DISCUSSION

Changes in Kerogen Composition During Maturation

Pyrolysis gas chromatography was used to evaluate the composition of kerogens at different levels of thermal maturation. Results are shown in Table 3. Multistep pyrolysis gas chromatography was performed using the lowest maturity sample of the Tithonian source-rock sequence E 41495 (well A, 0.35% R_o).

The naturally maturated series was dominated by aliphatic compounds, namely n-alkane/alkene doublets followed by alkyl-benzenes and alkyl-naphthalene's, alkyl-hyphens, and isoprenoids. The highest individual compound yields were measured in the gas range (C_1–C_5) followed by intermediate molecular weight compounds (C_6–C_{14}) and higher molecular weight compounds (C_{15+}). Alkyl-thiophenic compounds were abundant in the low-maturity samples, but their yields clearly decreased with increasing sample maturity (Figure 2). In the naturally maturated series, the first compounds to disappear were the isoprenoid thiophenes, which were no longer detectable in samples with maturities above 0.57% R_o. A series of C_5–C_{12} alkyl-thiophenes with an isoprenoid side chain were tentatively identified and quantified using GC-MS by summing the principal fragments m/z 97 + 98, 111 + 112, 125 + 126, and 139 + 140. Among these, the principal ion fragment was that of 2,5-dialkyl-thiophene (m/z 111 + 112), which represented nearly 20% of the total content. This suggests that sulfur-containing moieties are released at low levels of

Table 3. **Pyrolysis gas chromatography data from nine Tithonian sourcE-rock samples. Well locations are shown in Figure 1.**

Well	*A*	*B*	*C*	*D*	*F*	*H*	*I*	*J*	*K*
Totals: mgHC/g TOC	*E41495*	*E41502*	*E41525*	*E41449*	*E41459*	*E41488*	*E41440*	*E41500*	*E41509*
Total	595.75	564.18	511.38	304.36	174.29	241.65	64.63	81.91	16.77
C_{1-5}	57.17	74.92	67.05	60.47	40.58	52.74	13.59	27.67	7.29
C_{6-14}	164.95	155.18	140.77	103.10	66.97	78.61	26.76	25.60	4.69
C_{15+}	373.63	334.07	303.56	140.79	66.74	110.29	24.28	28.65	4.79
C_{6+} (total)	538.59	489.26	444.33	243.89	133.71	188.90	51.04	54.25	9.48
TR*	0.00	0.23	0.39	0.56	0.77	0.77	0.95	0.96	0.98

**Transformation ratio*

maturity, consistent with the generation of sulfur-rich oil at lower maturities (di Primio and Horsfield, 1996). Absolute quantities of alkylbenzenes and light molecular weight aliphatics also decreased through maturation but increased relative to the alkyl-thiophenes (Figure 2).

For the multistep pyrolysis experiments, highest yields were measured for the temperature range of 375° to 450°C (three of the steps mentioned above), where 65% of the total yield was generated in a 75°C temperature interval. The first step, which also involved a temperature increase of 75°C, led to the generation of 22% of the total yield, whereas the final step from 450–600°C produced only 13% of the total yield (Figure 3). In the five steps performed in the multistep PyGC experiment, the highest yield was always observed for the C_1–C_4 range, which showed a relatively constant increase with increasing pyrolysis temperature. Methane, which maximized in the last heating stage (450–600°C), had the highest individual yield. The C_{6+} fraction showed increasing yields up to 450°C, after which the yields decreased drastically. The highest proportion of alkyl-thiophenes was generated in the first step of the experiment (300–375°C), where the highest yields of benzo-thiophenes and alkylbenzenes also were observed. The second heating step was characterized by the maximum generation of C_{15+}*n*-alkanes/alkenes, alkylnaphthalenes, and isoprenoids. In the third heating step (400–425°C), *n*-alkanes/alkenes in the range C_2–C_{14} reached their highest yields (Figure 3). All pyrolysates generated in this multistep experiment were characterized by the predominance of *n*-alkane/alkene doublets. The low temperature pyrolysates were characterized additionally by abundant alkyl-thiophenic compounds, whereas short-chained alkenes and alkanes dominated the pyrolysate composition at higher temperatures. This confirms observations from the natural maturation series. di Primio and Horsfield (1996) used a low maturity sulfur-rich source rock to perform such a multistep PyGC experiment and showed the same general compositional change as a function of the pyrolysis temperature. However, they also reported kinetic parameters on the same sample and correlated these to the pyrolysate composition. They attributed the generation of thiophenic compound-rich pyrolysates at relatively low levels of thermal stress to the relatively easy cracking of sulfur-carbon bonds.

Changes in Gas-oil Ratio from Open-System Pyrolysis

The total gas-to-oil ratio (GOR) (ratio of C_1–C_5 to C_{6+} determined on the total pyrolysate after blank subtraction) (kg/kg) was determined for nine Tithonian source-rock samples. The low-maturity samples showed GORs of 0.11 to 0.14, the mature samples ranged from 0.25 to 0.34, and the high-maturity samples showed GORs from 0.51 to 0.75 (Figure 4). The trend of GOR versus vitrinite reflectance in Figure 5 indicates that the GORs of fluids generated during the maturity interval corresponding to the oil window remain relatively constant, and only at advanced maturity stages do GORs increase significantly (see also Düppenbecker and Horsfield, 1990). It should be noted that all of the above refers to remaining GOR, i.e. GOR for maturity levels above that of the sample. For a petroleum system in which all fluids and gases generated from the source rock are trapped, the impact of the high-GOR fluids can be assumed to be small, regionally speaking, because the high-GOR fluids are generated only in very low proportions. In this regard, pyrolysis yield of the highest maturity sample accounted to only 3% of the yield of the lowest maturity sample. It should be noted that

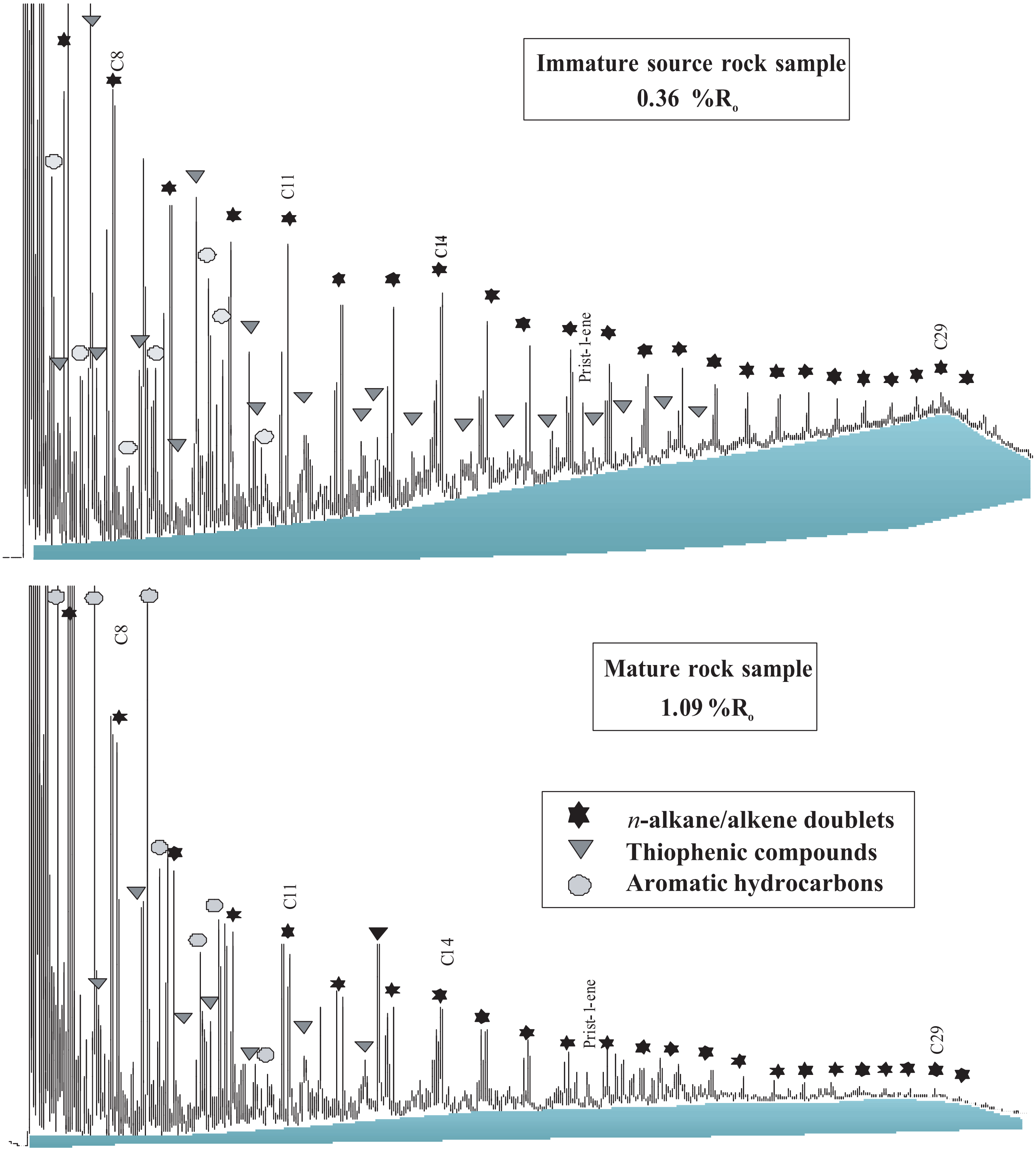

Figure 2. Gas chromatography (GC) traces of two Tithonian kerogen concentrates representing extremes of sample maturity in which thiophenic compounds were monitored.

the very low GORs of the immature samples are caused by the significant contribution of the unresolved "hump" of these pyrolysates. If only the resolved components above the hump are considered, GOR values are higher overall (also see Düppenbecker and Horsfield, 1990; Horsfield, 1997), varying between 0.4 and 2.1 kg/kg.

The GOR of the resolved compounds (GOR_{Res}), as well as of the total generated products, including the unresolved hump (GOR_{Tot}) of the pyrolysates

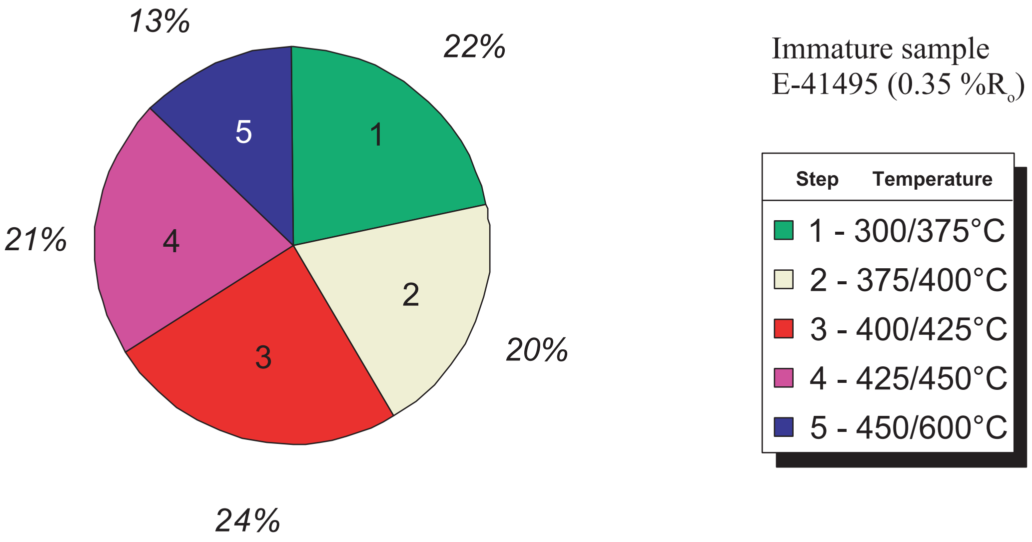

Figure 3. Pyrolysate total hydrocarbons (in percent) generated during multistep pyrolysis of the immature Tithonian source-rock sample. The total yield of this experiment was 552 mg HC/g TOC.

generated in the multistep experiment, are shown in Figure 6. For both GOR relationships, an increase with pyrolysis temperature was recorded. The increase of the resolved GOR, however, was much stronger than for the GOR calculated on total pyrolysate composition, and the extrapolation of this type of data to a natural maturity sequence is difficult because laboratory experiments cannot take migration into account. In general, the GOR$_{\mathrm{Tot}}$ tends to be too conservative as compared to natural samples, whereas the

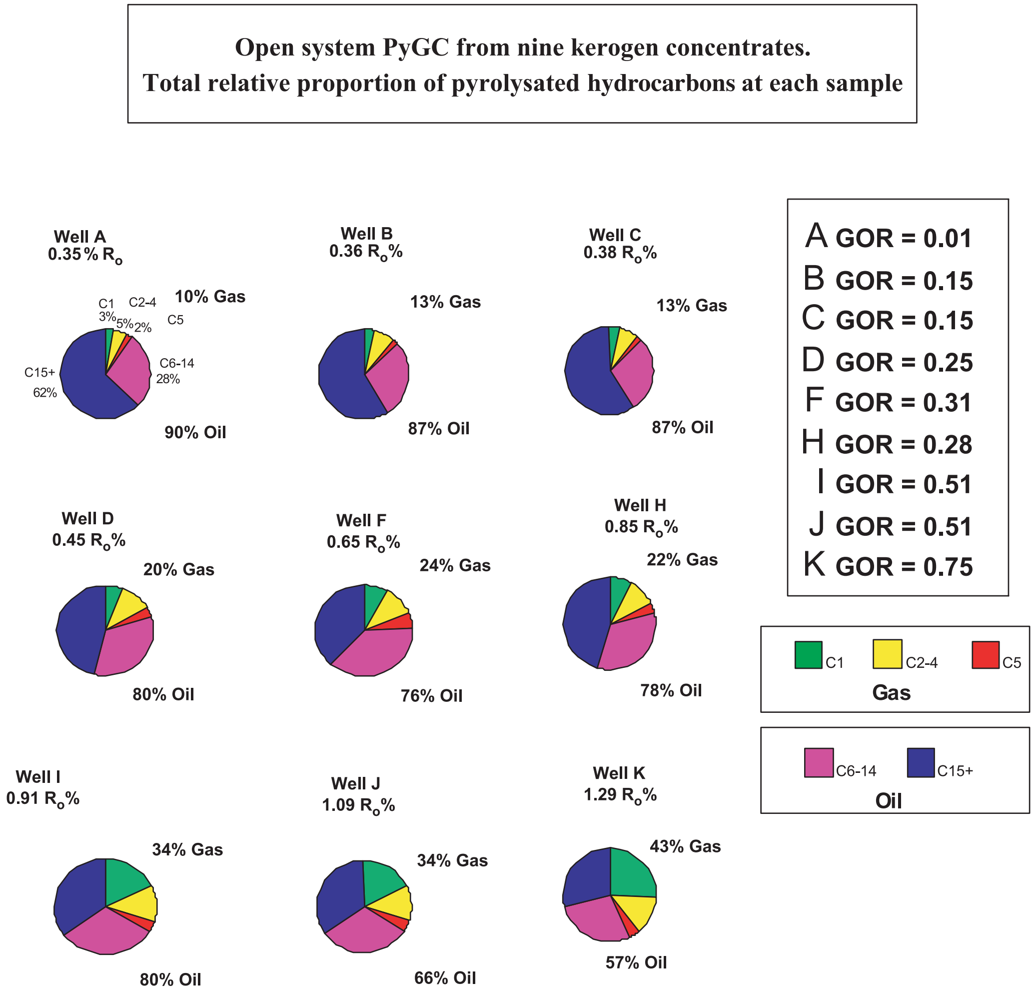

Figure 4. Composition of the pyrolysates generated from the maturity sequence of Tithonian source rocks analyzed. Sample maturity increases from upper left to lower right in this figure.

Figure 5. Total gas-oil ratio (GOR) of the sequence of Tithonian source rock samples analyzed by PyGC as a function of sample maturity.

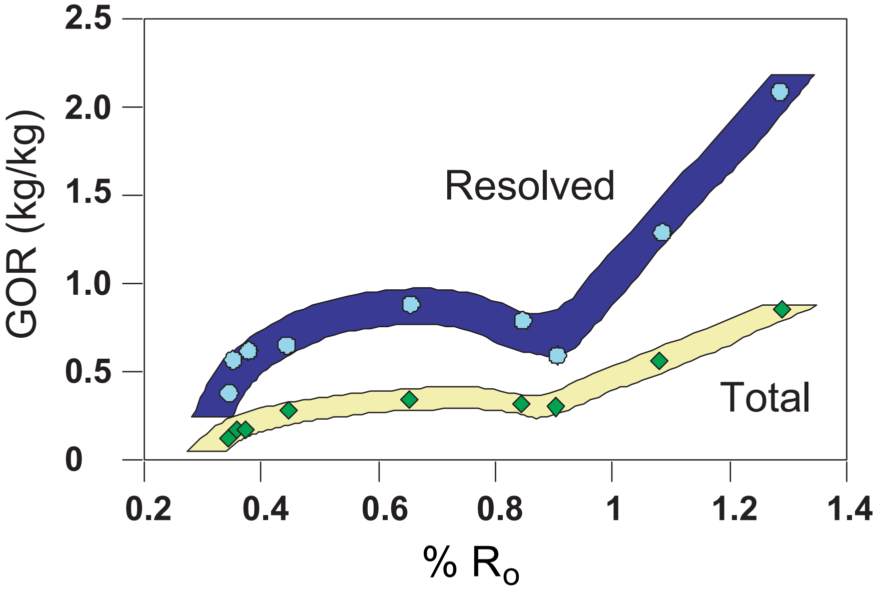

GOR$_{Res}$ tends to be too high as compared to naturally occurring fluids (Düppenbecker and Horsfield, 1990). This has been confirmed to some degree by PVT modeling of petroleum fluids in the North Sea (di Primio et al., 1998, and personal communication, 2002); most of the pyrolysis hump has to be excluded in order to obtain a good fit.

Simulation of Maturation Using MSSV Pyrolysis

In order to model product compositions as a function of maturity (using basin modeling techniques, for example), simulation rather than analytical pyrolysis methods usually are employed. There are two common approaches. The first is to directly determine kinetic constants for the generation of individual compounds, compositional classes, or boiling ranges (e.g., Espitalié et al., 1988; Dieckmann et al., 2000). The second is simply to relate product compositions to transformation ratio (TR), and to predict TR using bulk kinetic models (e.g., Düppenbecker and Horsfield, 1990). Relating product compositions to TR has been employed here.

The same sample used for the multistep PyGC experiment also was subjected to artificial maturation in a closed system using the MSSV technique developed by Horsfield et al. (1989). For this experiment, a total of seven heating stages from 300 to 450°C (0.7 Kelvin/min) were used. In this case, and unlike the measurements from PyGC, cumulative compositions were determined (Figure 7).

Product Compositions and Gas-to-oil Ratios

Product yields increased from 13 to 489 mgHC/g TOC with increasing temperature. The pyrolysates

Figure 6. Calculated GOR relationships based on resolved fluid composition and total pyrolysate composition of the pyrolysates generated in the course of the multistep PyGC experiment.

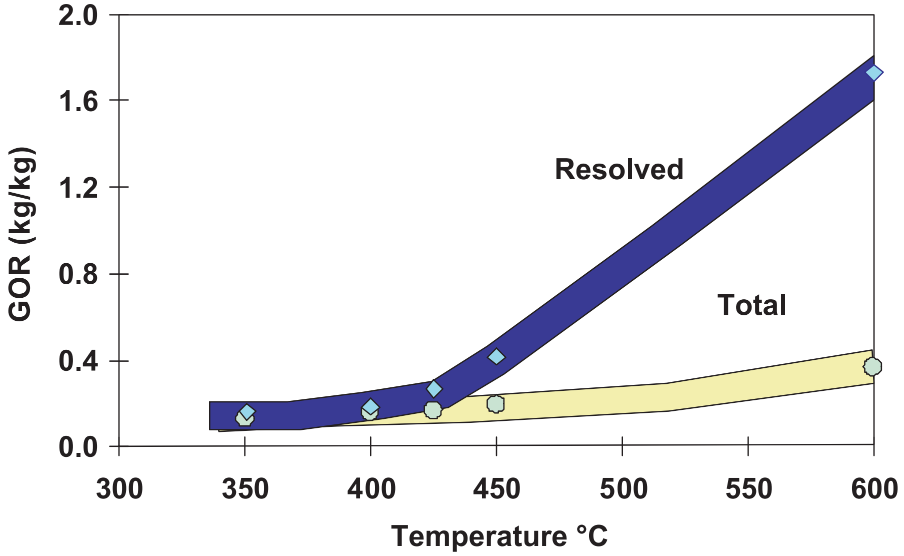

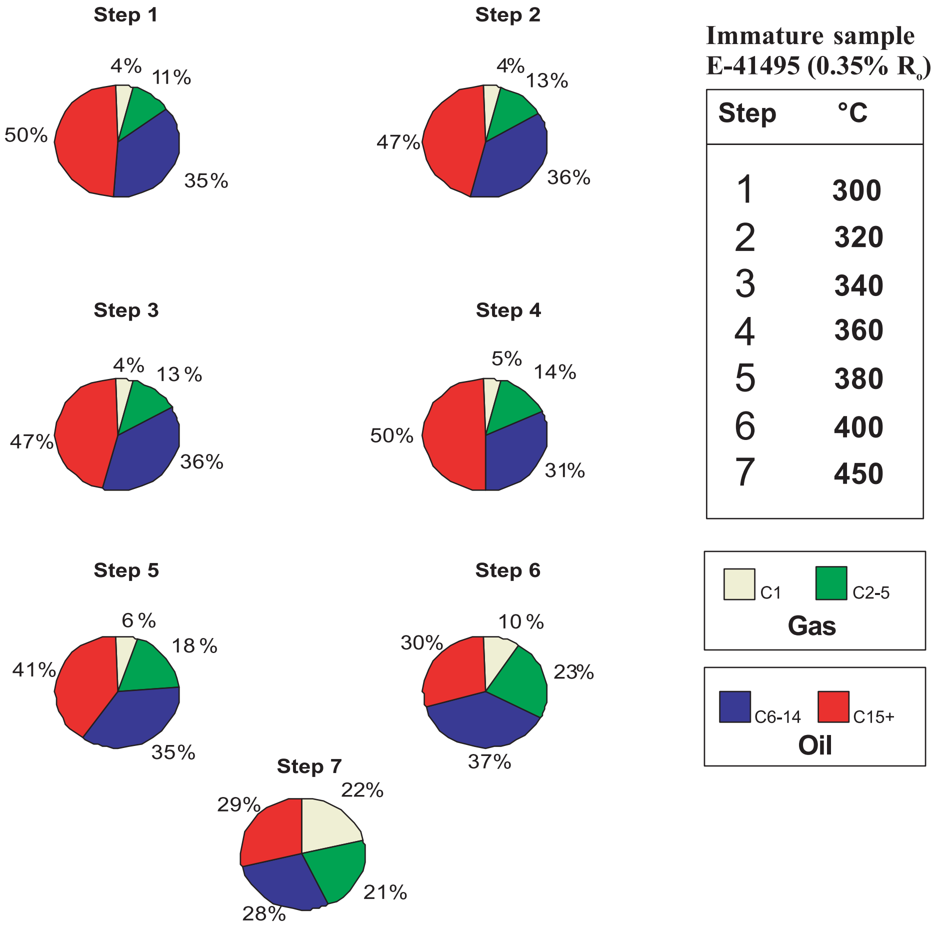

Figure 7. Composition of the pyrolysates generated during a microscale sealed-vessel pyrolysis (MSSV) experiment on the immature source-rock sample. The sample was heated in seven steps at a range of 300° to 450°C.

were dominated by *n*-alkanes of low molecular weight (n-C_1 to n-C_5) followed by alkyl-thiophenes and intermediate molecular weight *n*-alkanes (n-C_6 to n-C_{14}). Isoprenoids occurred only up to 400°C and were no longer recognizable at experimental temperatures above 360°C. The alkyl-thiophene (T) series from C_7-T to C_{12}-T (?) appeared from 340°C, which supports the proposition that these compounds are generated through functional group rearrangement (Koopmans et al., 1995). The highest individual yield always was observed for methane followed by ethane through butane, meta-para-xylene and C_5 to C_7 alkanes. Only in the first two steps do thiophene and 2 methyl-thiophene dominate over the other C_{5+} compounds. With increasing pyrolysis temperature, C_3 and C_4 thiophenes increased to nearly match the benzothiophene yields. Toluene showed the highest yield among the aromatic compounds at all temperatures. *n*-alkenes were not observed in the products of these MSSV experiments. The cumulative GOR based on total products remained more or less constant and below 0.11 for transformation ratios up to about 0.8, above which GOR increased to 0.36 because of secondary cracking. GOR based on resolved components essentially remained constant at about 0.22 until secondary cracking thereafter raised values to 1.20.

Calibration by Compositional Mass-balance Modeling

The predictions of cumulative GOR from MSSV pyrolysis were evaluated with a calibration exercise using the natural maturity series from the Sonda de Campeche. In this regard, Horsfield et al. (2001) presented a compositional mass-balance model for petroleum formation based on pyrolysis gas chromatography and Rock Eval data for maturation series. Briefly, the model has the following elements (see Appendix 1 for more details):

1) calculation of TR from Rock Eval data using the algebraic scheme of Pelet (1985),
2) gathering of quantitative pyrolysis gas chromatography data,
3) normalization of data to original TOC (prior to generation and expulsion), and

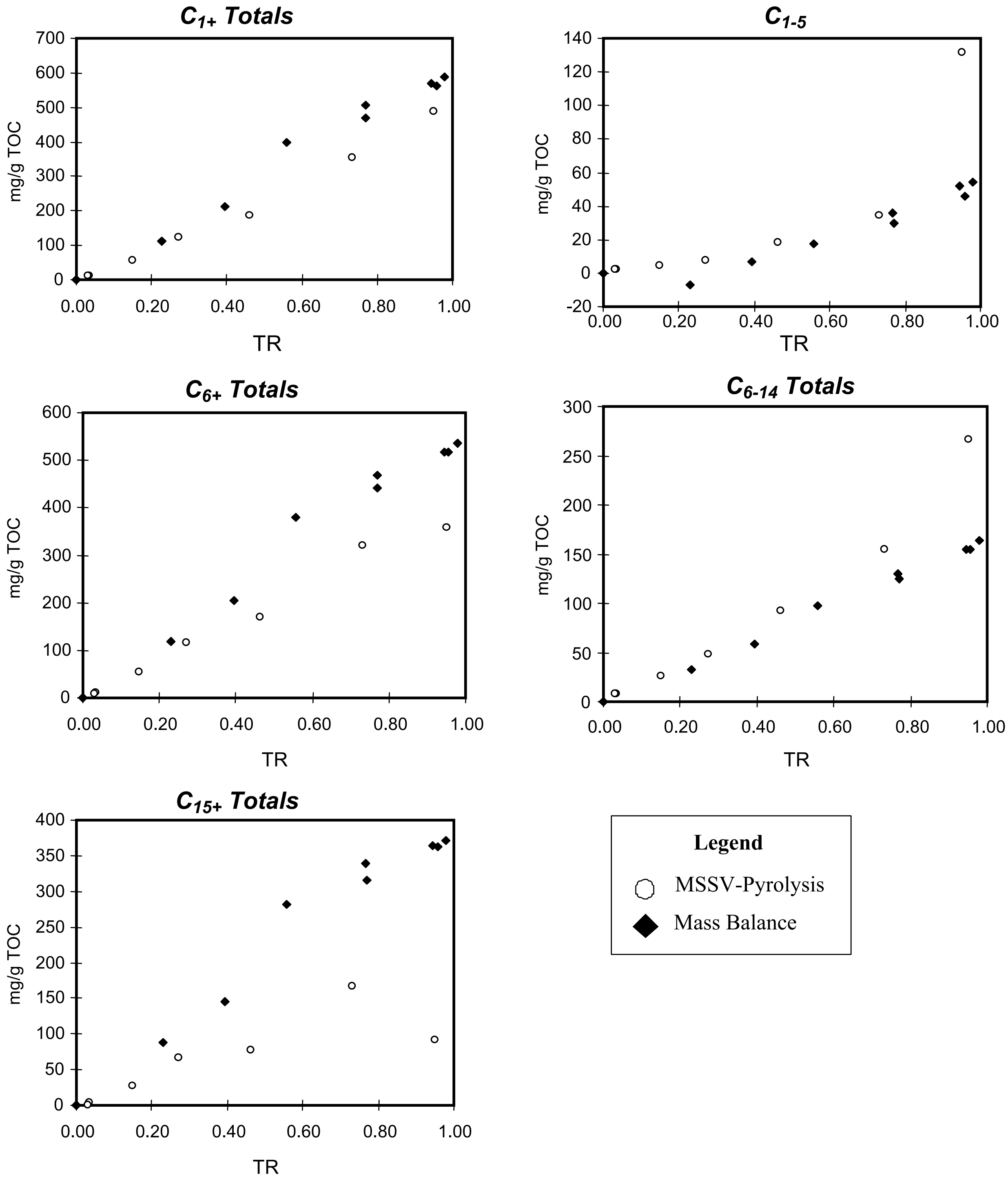

Figure 8. Calculated GOR relationships based on resolved fluid composition and total pyrolysate composition of the pyrolysates generated during an MSSV experiment on an immature Tithonian source-rock sample.

4) calculation of principal component yields by subtracting normalized yields from that of the least mature sample in the series.

Figures 8, 9 and 10 show the product yields versus TR from mass balance and as measured directly from MSSV pyrolysis. Bulk fractions, compound classes, and single compounds are displayed. The correspondence between the two data sets is very good, considering the potential errors involved in measurements and in the assumptions of the mass-balance model. Some features stand out: production of alkylaromatics by

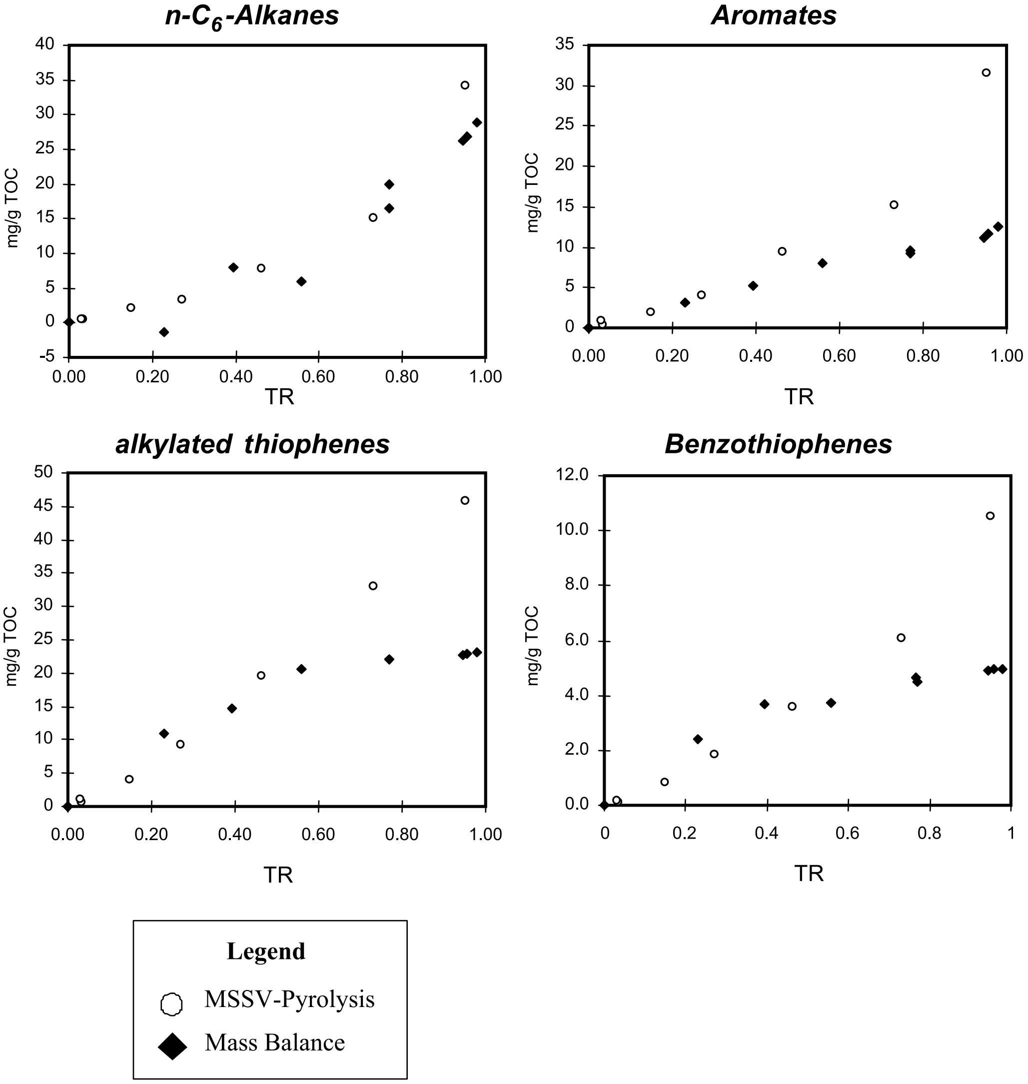

Figure 9. The product yields versus transformation ratio (TR) from mass-balance modeling and as measured directly from MSSV pyrolysis. The production of fraction hydrocarbons that were generated during an MSSV experiment of the immature Tithonian source rocks is compared with the production of fraction hydrocarbons derivative of PyGC of the natural maturity series.

means of secondary reactions occurs above a TR of 0.6 for MSSV pyrolysis, a feature that is not seen in the natural series. Normal alkanes (n-C_{6+}), on the other hand, show a remarkably close fit, even with very high TR values. As far as cumulative GOR is concerned, those from PyGC mass-balance predictions are slightly lower than those from MSSV pyrolysis, mainly because the former have a higher proportion of unresolved C_{6+} components.

Comparison with GOR from Field Data

Field GOR data from the Sonda de Campeche are given in Table 4. Values have been converted from oil field units (scf/bbl, m^3/m^3) into mass units directly comparable with laboratory measurements. GOR increases in a general northeast-to-southwest direction, thereby paralleling the regional maturity pattern. The trend shows a strong similarity to that of successive PyGC determinations with increasing rank, rather than with estimates of cumulative GOR based on either the PyGC mass-balance model or MSSV pyrolysis.

This finding indicates that the Sonda de Campeche, while a textbook example of a vertically drained "supercharged, high impedance petroleum system" (Demaison and Huizinga, 1994), is not one where cumulative filling of traps occurs. In this regard, we earlier reported how molecular maturity parameters exhibited similar behavior (Santamaria et al., 1998), and we proposed that less mature petroleum in the northeast might have been trapped synchronously with higher maturity petroleum farther to the southwest, with low-maturity petroleum formed prior to trap formation in the southwest having been dissipated. Trap formation resulting from salt movement and growth faulting might have taken place in the late Miocene, whereas petroleum generation could have

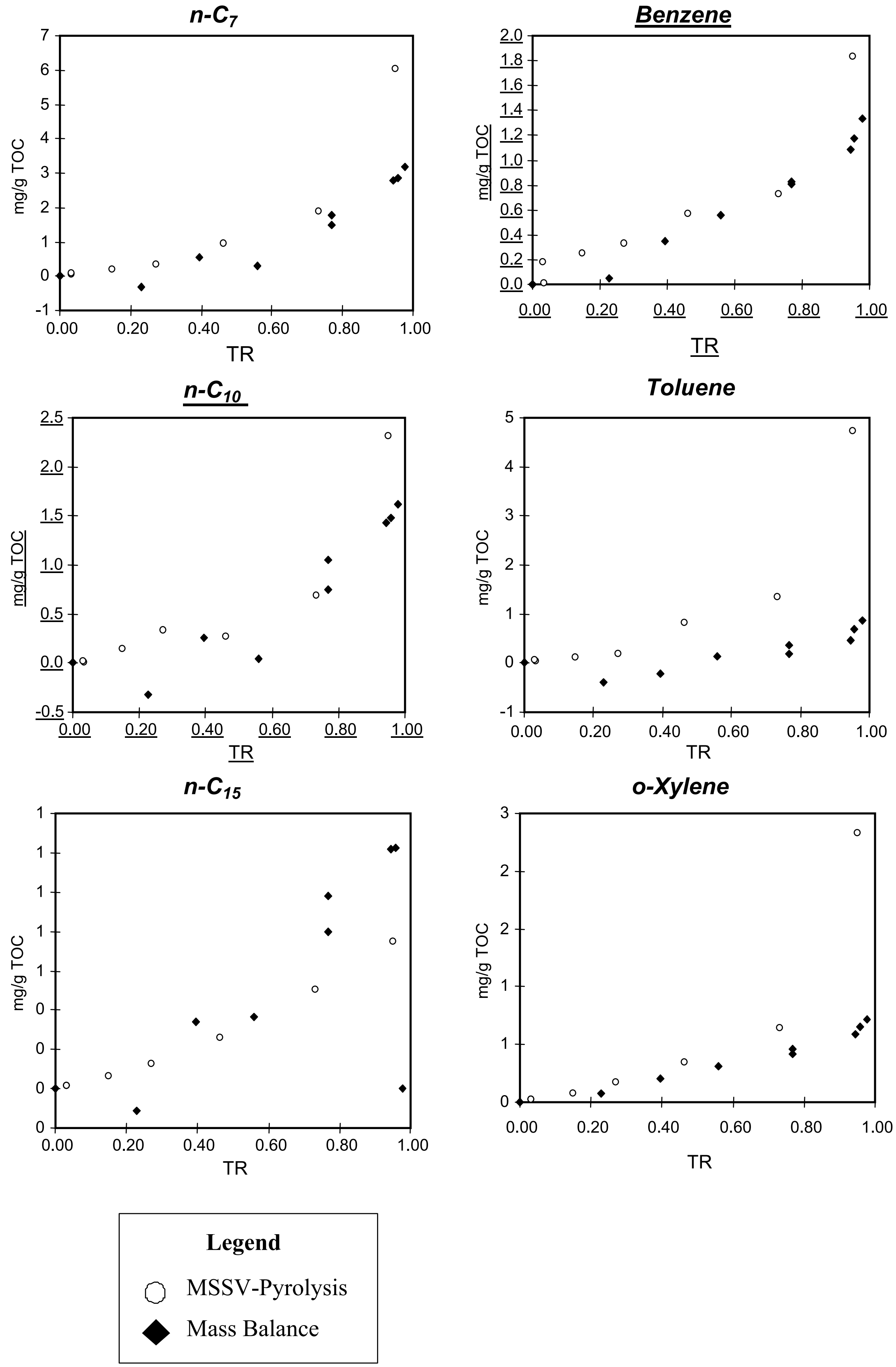
n-C7
mg/g TOC
7
6
5
4
3
2
1
0
-1
0.00
0.20
0.40
0.60
0.80
1.00
TR
Benzene
2.0
1.8
1.6
1.4
1.2
1.0
0.8
0.6
0.4
0.2
0.0
n-C10
2.5
2.0
1.5
1.0
0.5
0.0
-0.5
Toluene
n-C15
o-Xylene
Legend
MSSV-Pyrolysis
Mass Balance

Table 4. Field GOR data for the Sonda de Campeche, with values expressed in kg/kg.

GOR kg/kg	Field Name	Offshore
0,09	Maloob	NE
0,17	Ku	
0,22	Ku (?)	
0,14	Zaap	
0,18	Nohoch	
0,13	Chac	
0,18	Akal	
0,19	Kanaab	
0,27	Citam	
0,36	Taratunich	
0,25	Abkatun	
0,37	Batab	
0,28	Pol	
0,42	Chuc	
0,80	Och	
0,73	Uech	
0,81	Bolonticub	
1,09	Yum	SW

occurred throughout the Miocene, possibly before trap formation in some instances, in the southwest Sonda de Campeche (Holguín, 1987; Angeles-Aquino, 1994).

CONCLUSIONS

The Tithonian source rocks from the Sonda de Campeche cover the entire oil window and have generated sulfur-rich oil and gas. Regional field GOR trends are consistent with instantaneous rather than cumulative GOR predictions in mass-balance and artificial maturation experiments, thereby supporting the notion of mainly localized vertical migration avenues in association with a late timing of trap formation.

ACKNOWLEDGMENTS

We want to acknowledge the support of the Institute of Petroleum and Organic Geochemistry (ICG-4) of Forschungszentrum Jülich, Germany; the Marine Region Exploration division of Mexican Petroleum (Pemex); and the Exploration Division of the Mexican Petroleum Institute (IMP). Personal thanks are extended to Rolando di Primio for valuable discussions; to Franz Leistner and Maria de Jesús Saucedo-García for expert technical support; to María A. Romero-Ibarra, Noel Holguín-Quiñones, and Baldomero Carrasco-Velázquez, who authorized the supply of rock samples and geological information; and to Dietrich H. Welte and Raúl Gonzáles-García (formerly with ICG-4 and Pemex, respectively) who initiated this cooperation between the Mexican and German partner organizations.

APPENDIX 1
ELEMENTS OF THE COMPOSITIONAL MASS-BALANCE MODEL (AFTER HORSFIELD ET AL., 2001)

Calculation of Transformation Ratio (Pelet, 1985)

$$TR = [1200 \times (HI_o - HI_x)]/[HI_o \times (1200 - Hi_x)]$$

where

HI_o = Hydrogen index of immature sample
HI_x = Hydrogen index of mature sample
1200 represents the reciprocal (times 1000) of 0.83, the assumed proportion of carbon in Rock-Eval pyrolysis products

Gathering of thermal analysis data

Boiling ranges C_1–C_5, C_6–C_{14}, and C_{15+}, chromatographically resolved (skim integration) components in the C_6–C_{14} and C_{15+} ranges, summed and individual *n*-alkanes and *n*-alkenes in the range *n*-C_6–*n*C_{30} were quantified using an external *n*-butane standard.

Normalization of thermal analysis data

PyGC data, normalized to the current TOC content, must be renormalized to the original TOC of the sample before generation and migration take place. Pelet (1985) showed that for total petroleum yields, the normalization is expressed by:

$$HI_i = [HI_x \times (1200 - HI_o)]/(1200 - HI_x)$$

Figure 10. The product yields versus TR from mass-balance modeling and as measured directly from MSSV pyrolysis. The production of single compounds that were generated during an MSSV experiment on the immature Tithonian source rock is compared with the production of single compounds derivative of PyGC of the natural maturity series.

Therefore, for any given component with a measured concentration N_x from PyGC analysis, the initial concentration N_i is given by:

$$N_i = [N_x \times (1200 - HI_o)]/(1200 - HI_x)$$

Calculation of component yields

For the least mature sample in the series, renormalization is not necessary, as its value N_o represents the unmatured starting point with which all other samples are compared. Just as hydrogen indices decrease during maturation, so do most measured and normalized yields of individual components. The actual decrease corresponds to the yield of that component that is generated from the kerogen during maturation. This yield is given by $(N_o - N_i)$ and changes as a function of TR.

For calculating the TR, total pyrolysis product (C_{1+}) yields are measured from sample aliquots during programmed temperature pyrolysis (e.g., 0.7 min/min). TR is defined as the ratio of the yield divided by the maximum yield measured at the cumulative plateau. Yields of individual compound classes are quantified directly.

REFERENCES CITED

Angeles-Aquino, F. J., 1987, Estudio Estratigráfico-Sedimentológico del Jurásico Superior en la Sonda de Campeche: Ingeniería Petrolera AIPM, v. 28, no. 1, p. 45–55.

Angeles-Aquino, F. J., 1994, Tectonic evolution, structural styles, and oil habitat in the Sonda de Campeche, Mexico: AAPG Bulletin, v. 78, p. 1448–1449.

Demaison, G. J., and B. J. Huizinga, 1994, Genetic classification of petroleum systems using three factors: Charge, migration and entrapment, *in* L. Magoon and W. G. Dow, eds., The petroleum systems from source to trap: AAPG Memoir 60, p. 73–89.

Dieckmann, V., B. Horsfield, and H. J. Schenk, 2000, Heating rate dependency of petroleum-forming reactions: Implications for compositional kinetic predictions: Organic Geochemistry, v. 31, no. 12, p. 1333–1348.

di Primio, R., and B. Horsfield, 1996, Predicting the generation of heavy oil in carbonate/evaporitic environments using pyrolysis methods: Organic Geochemistry, v. 24, p. 999–1013.

di Primio, R., V. Dieckmann, and N. Mills, 1998, PVT and phase behavior analysis in petroleum exploration: Organic Geochemistry, v. 29, p. 207–222.

Düppenbecker, S. J., and B. Horsfield, 1990, Compositional information for kinetic modelling and petroleum type prediction, *in* B. Durand and F. Behar, eds., Advances in organic geochemistry 1989: Organic Geochemistry, v. 16, p. 259–266.

Durand, B., and G. Nicaise, 1980, Procedures for kerogen isolation, *in* B. Durand, ed., Kerogen: Paris, Technip, p. 35–53.

Espitalié, J., P. Ungerer, I. Irwin, and F. Marquis, 1988, Primary cracking of kerogens. Experimenting and modelling C_1, C_2-C_5, C_6-C_{15} and C_{15+} classes of hydrocarbons formed: Organic Geochemistry, v. 13, p. 893–899.

González, G. R., and Q. N. Holguín, 1991, Geology of the source rocks of Mexico, Source-Rock Geology, *in* XIII World Petroleum Congress, Topic 2, Forum with Posters, Buenos Aires, Argentina, p. 1–10.

González-G., R., and N. Holguín-Q., 2001, Las rocas generadoras de México: Boletín Asociación Mexicana Geólogos Petroleros, v. 49, no. 1–2, p. 16–30.

Holguín-Q., N., 1987, Evaluación Geoquímica del Sureste de México: Boletín Asociación Mexicana Geólogos Petroleros, v. 37, no. 1, p. 3–48.

Horsfield, B., 1997, The bulk composition of first-formed petroleum in source rocks, in D. H. Welte, B. Horsfield, and D. R. Baker, eds., Petroleum and basin evolution: Berlin, Springer-Verlag, p. 335–401.

Horsfield, B., and S. J. Düppenbecker, 1991, The decomposition of Posidonia Shale and Green River Shale kerogens using microscale sealed vessel (MSSV) pyrolysis: Journal of Analytical Application of Pyrolosisosis, v. 20, p. 107–123.

Horsfield, B., U. Disko, and F. Leistner, 1989, The microscale simulation of maturation: Outline of a new technique and its potential applications: Geologische Ründschau, v. 78, no. 1, p. 361–374.

Horsfield, B., V. Dieckmann, D. Santamaría-Orozco, D. J. Curry, and H. J. Schenk, 2001, Compositional mass balance of petroleum formation (Abs.): 20th International Meeting of Organic Geochemistry (EGOA), Nancy, France, September 10–14, P-THU3-14.

Koopmans, M. P., J. S. Sinninghe-Damsté, M. D. Lewan, and J. de Leeuw, 1995, Thermal stability of thiophene biomarkers as studied by hydrous pyrolysis: Organic Geochemistry, v. 23, no. 6, p. 583–596.

Ortega-L., S., M. Guzmán-V., L. Medrano-M., and L. Clara-V., 1996, La ventana de generación del subsistema generador Tithoniano en la Sonda de Campeche (Abs.): 5th Latin-American Congress of Organic Geochemistry, Cancún, Mexico, p. 203–204.

Ortuño, M. E., 1999, El Tithoniano formación productora de Hidrocarburos en la Sonda de Campeche: Ingeniería Petrolera, v. 39, p. 29–37.

Pelet, R., 1985, Évaluation quantitative des produits formés lors de l'évolution géochemique de la matière organique: Revue de l'Institut Français du Pétrole, v. 40, p. 551–561.

Romero-I., M. A., M. J. Ruiz, M. L. Medrano, G. J. Durán, R. R. Rojas, M. I. Gutiérrez, and C. J. Baltazar, 1999, El Sistema Petrolífero Tithoniano-Cretácico (!) en el Área

Marina de Campeche, México (Abs.): 3^a Conferencia Internacional Conjunta Asociación Mexicana de Geólogos Petroleros/AAPG, October 10–13, Veracruz, México, p. PS-7.

Santamaría-Orozco, D., R. di Primio, W. Pickel, N. Holguín, and B. Horsfield, 1995, Organic facies and maturity of Tithonian Source Rocks from the Sonda de Campeche, Mexico, *in* J. O. Grimalt and C. Dorrosoro, eds., Developments and applications to energy, climate, environment and human history: Selected papers from the 17th International Meeting of Organic Geochemistry (EGOA), San Sebastian, Spain, p. 152–154.

Santamaría-Orozco, D., R. di Primio, and B. Horsfield, 1997, Eustatic controls of source rocks deposition in the Tithonian of the Sonda de Campeche (Abs.): 18th International Meeting of Organic Geochemistry (EGOA), Maastricht, The Netherlands, September 22–26, p. A60.

Santamaría-Orozco, D., R. di Primio, B. Horsfield, and D. H. Welte, 1998, Influence of maturity on sulphur-compounds in Tithonian source rocks and crude oils, Sonda de Campeche, Mexico: Organic Geochemistry, v. 28, p. 423–439.

Sosa, P. A., 1995, Hipótesis del inicio de la ventana de petróleo para el kerógeno II-II-S de las Cuencas Terciarias del Sureste de México: Ingeniería Petrolera de Asociación de Ingenieros Petroleros de México, v. 36, no. 3, p. 47–58.